Deterministic DNA barcoding using vacuum-driven loading of free oligonucleotides to microwell arrays

Patrycja Baranowska[1], Trinh Lam[2], Amy E. Herr[2,3]*

[1]Centre for Advanced Materials and Technologies CEZAMAT, Warsaw University of Technology, Warsaw, Poland

[2]University of California, Berkeley, USA

[3]Chan Zuckerberg Biohub, San Francisco, USA

Keywords: microfluidic systems, barcoding, vacuum-driven, passive flow, high-throughput, deterministic

Abstract

Achieving high-throughput and cost-effective next-generation sequencing requires sample (samples, cells/beads) pooling. A key approach to pooling samples while maintaining unambiguous sample identification is to employ DNA barcoding, which assigns each specimen a unique nucleotide (index) sequence. For barcoding in droplets and microwells, one widely used approach is to randomly seed a unique oligo-coated bead into each compartment. Synthesis of oligonucleotide-coated beads (e.g., split-pooling) is exceptionally intensive and random seeding can result in errors. As an alternative, we present deterministic, aqueous barcoding of 512 arrayed

microwells using a multi-layer, vacuum-driven microfluidic network. To uniquely barcode each of the 512 microwells, the oligonucleotide solutions are designed using a Combinatorial Dual Indexing (i5, i7) scheme with the deterministic loading. Deterministic loading of the solutions is achieved by sequentially mating two bifurcated and complementary microchannel-network layers to the microwell array. Vacuum-assisted flow and dead-end channel design yields uniform barcode patterning in the microwell array (~20% CV), reasonable barcode loading times (30 - 40 min per one step), and reduced reagent use (~ 8-16 μL at 25 μM oligos vs. 10-50 μL at 100 μM for bead systems). Cross-contamination occurred in ~4% of the microwells, well within the acceptable range. Following DNA barcode delivery, on-chip PCR of nuclear DNA from a breast cancer cell line having the characteristics of the differentiated mammary epithelium (MCF7) was successfully performed, with off-chip quality control of the amplified breast cancer DNA. Overall, we describe a deterministic and bead-free DNA barcoding strategy for efficient barcoding of widely used microwell arrays.

Introduction

The development of sequencing technologies has transformed the scale and efficiency of genomics.[1] Contemporary next-generation sequencing (NGS) platforms routinely generate billions of reads per run, and this throughput is made possible in part by barcoding, where each library is given its own unique barcode that acts as a sample tag, allowing traceability from the NGS readout back to the original cells or samples.[2] Barcoding reduces costs and turnaround times, with each readout accurately traced back to the originating cell, even with pooling.[3] One of the most widely used strategies for barcoding is bead-based barcoding, in which uniquely labelled beads capture

RNA or DNA from individual cells or nuclei.[4–6] These methods are most commonly implemented in two forms: droplet-based and microwell-based. In droplet-based approaches, individual cells or nuclei are encapsulated within microdroplets containing barcoded beads and lysis buffer (10x Genomics Chromium[7], Drop-seq[1], inDrops[8]). In microwell or plate-based approaches (e.g., Smart-seq2[9], Seq-Well[10], sci-RNA-seq[11]), cells are deposited into wells seeded with magnetic beads with unique barcodes; upon cell lysis, RNA or DNA binds to the bead, thus precisely assigning resultant transcripts to individual cells, while the magnetic properties of the beads allow for convenient isolation and downstream processing.[12] Despite advantages and widespread use bead-based methods have limitations, including the random assignment of barcodes, high costs, bead aggregation, additional steps in barcode preparation and loss of material during magnetic separation, some of which may be exacerbated by the application of a magnetic field.[13–16]

An alternative approach is the aqueous barcode strategy in which barcodes are delivered in solution rather than immobilized on beads.[17] Aqueous DNA barcodes provide greater flexibility in barcode design and facilitates combinatorial indexing to generate a unique combination of nucleic acid barcodes for each cell, although aqueous barcodes require careful control of fluid delivery to prevent barcode cross-contamination (i.e., diffusion, mixing). One powerful implementation is Combinatorial Dual Indexing (CDI), which creates a large set of unique barcodes by combining a small pool of, for example, the i5 and i7 dual-index barcodes for Illumina NGS (e.g., 8 of i5 × 12 of i7 = 96 unique pairs for a standard 96-well plate).[11] In microfluidic systems, CDI allows deterministic assignment of barcodes in a spatially organized grid, ensuring precise single-cell tracking, high throughput, and integration of transcriptomic or epigenetic data with spatial context.[18,19] The present work was inspired by the deterministic barcoding technique adopted by DBiT-seq[18,20], where parallel microfluidic channels deliver two barcode sets to tissue sections

resulting in grid-patterning of uniquely coded pixels across each tissue slice for spatial transcriptomics; its extension, xDBiT[21], supports simultaneous analysis of multiple tissue sections while preserving high-spatial resolution.

Inspired by fluidic grid patterning[22,23] and CDI deterministic barcoding, we sequentially apply two vacuum-driven orthogonally oriented microchannel layers (horizontal and vertical) to pattern a unique DNA barcode in each microwell of a 512 microwell array. Unlike previously described systems[24–26], vacuum is generated by interfacing each microfluidic chip to suction from a house vacuum system. Importantly, we design the deterministic approach using aqueous DNA barcodes to eliminate resource-intensive synthesis and functionalization of beads with oligonucleotides. Concomitantly, aqueous barcode formulations reduce reagent consumption compared to existing protocols, thus reducing operational costs and biological material loss.[27] Here, we sought to harness the precision flow control afforded by microsystems to reduce microwell-to-microwell barcode cross-contamination. By combining high spatial resolution with operational simplicity and low instrumentation requirements, our platform offers an attractive and affordable alternative to current DNA barcoding techniques.[28]

Experimental Section

Choice of aqueous barcodes for combinatorial dual indexing of the microwell array

A combinatorial dual indexing (CDI) scheme was employed in conjunction with a deterministic barcode loading strategy to pattern each microwell of the 512 microwell array with a unique barcode index. We used Illumina i5 and i7 indexes as solution-phase barcodes. A 25-µM solution of the i5 barcode (Integrated DNA Technologies; in ultrapure water) was used for the horizontal loading step. Similarly, a 25-µM solution of the i7 barcode (Integrated DNA Technologies; in

ultrapure water) was used as the barcode for the vertical loading step. The barcode sequences are as follows:

i5	5'-AATGATACGGCGACCACCGAGATCTACACCTCTCTATTCGTCGGCAGCGTC-3'
i7	5'-CAAGCAGAAGACGGCATACGAGATCCGTTTAGGTCTCGTGGGCTCGG-3'

Device geometry and fabrication

The deterministic barcode loading strategy uses five PDMS-device layers: a 512 microwell array, a vacuum network, and three layers each consisting of different bifurcated microfluidic channel networks: a horizontal barcode delivery network, a vertical barcode delivery network, and a PCR reagent delivery network. Soft lithography was used to fabricate all layers: SU-8 3500 (Kayaku Advanced Materials) for horizontal, vertical, and PCR delivery layers, and SU-8 2100 for microwell and vacuum layers. Spin coating, soft baking, and PDMS development followed standard protocols (see SI). After each PDMS layer was cast, inlet holes were punched in the delivery layers (∅ = 1.5 mm) and the vacuum layer (∅ = 1 mm) using a biopsy punch. The vacuum layer had 4 ports connected to the house vacuum; the horizontal, vertical, and PCR layers had 16, 32, and 1 open ports, respectively.

Assembly of the multi-layer device and fluid routing for deterministic barcode loading

To assess microwell filling, we employed both brightfield and fluorescence imaging to visualize the microchannel-flow and microwell-filling characteristics. Imaging-based cross-contamination assessment used progressively more stringent test samples, progressing from solutions of

colorimetric (food) dyes, to fluorescein-o-acrylate (FITC acrylate, 1mg/ml in DMSO, Sigma-Aldrich), to finally solutions of oligonucleotides conjugated with fluorophores (biotin-i51-488 and oligo-A549, 25 uM in ultrapure water, Integrated DNA Technologies, IDT).

First, the microfluidic system was prepared, consisting of a square glass microscope slide (using as a stabilizing base layer), a PDMS layer with 512 microwells, a delivery layer (horizontal, vertical or PCR depending on the test), and a vacuum layer. The glass slide was thoroughly cleaned with isopropyl alcohol (IPA, Sigma-Aldrich), rinsed with a nitrogen stream (N_2), and subsequently the PDMS microwell-array layer was aligned and placed on it, ensuring the removal of any air bubbles. Next, the PDMS microwell layer was treated in an air plasma cleaner (PDC-32G, Harris Plasma) at a vacuum level of 0.470 Torr using an ICME pump, with the RF power set to High for 3 min. Subsequently, depending on the type of experiment (vertical loading, horizontal loading, or PCR loading), the microwell layer, delivery layer, and vacuum layer were aligned. Plasma activation combined with vacuum suction formed a temporary, leak-free seal between the layers, allowing both reliable operation and easy layer delamination and exchange for subsequent steps. All open inlets (16 for horizontal, 32 for vertical, and 1 for PCR membrane) were sealed with tape (600 Scotch Crystal, 3M), and vacuum was applied for ~1 min. During the vacuum application, the perimeter of the microwells was visually monitored for curvature (bowing) indicating evacuation of air from the microwells and resultant vacuum-force induced distortion of the microwell perimeter at the seal interface. Once bowing was visually observed, all inlets were opened and the barcode solution (biotin-i51-488, 25 uM in ultrapure water) was introduced to the inlets using a 20 μm pipette.

After fluid loading was complete, the vacuum layer was carefully removed. The microwell and inlet system was secured with non-adhesive side of PCR film (q225; Quantagene, KUBO) and the chip was centrifuged at 3000 RPM for 2 min.

Cross-contamination during deterministic loading of the microwell array

To assess potential cross-contamination between adjacent microwells, two solutions of oligonucleotide, with each oligonucleotide conjugated with distinct fluorescent tag, were prepared: oligo-A549 (Integrated DNA Technologies, IDT) and biotin-i51-488 (Integrated DNA Technologies, IDT) both in concentrations 25 uM prepared in ultrapure water. Biotin-i51-488 was used for the first barcoding step (horizontal) and oligo-A549 was used for the second barcoding step (vertical). The first barcoding step was performed by flowing Biotin-i51-488 solution to every second microchannel of the microsystem (channel pattern: oligo, water, oligo, water, etc.). In this way, horizontal rows of microwells were patterned with alternating solutions of fluorescent oligos and clear water. Fluid was introduced using a 20 µl pipette, followed by a 30-40 min loading duration. This alternating pattern allows ready visualization of any leakage of fluorescent solution between adjacent microwell rows. After all of the microwells were filled with the respective fluid, the vacuum layer was carefully removed, the microwell and inlet areas were sealed with q225 PCR sealing film (Quantagene, KUBO) and the system was centrifuged at 3000 RPM for 2 min. Fluorescence intensity in both the 488-nm and 549-nm spectral channels was measured across the microwell array.

Then, to prevent cross-contamination between microwells, the solution of oligonucleotides in the microwells were dried in an oven at 35°C for 15 min. The fluidic layer was then carefully removed, and the microwells were further dried at 35°C for 20 min. Next, the vertical delivery

layer was aligned to the microwell array layer containing the dried oligonucleotides. The vacuum layer was applied on top of the assembly, connected to the vacuum tubing, and all inlets were sealed with tape (600 Scotch Crystal, 3M). Vacuum was applied for ~1 min. Then the inlets were opened and oligo-A549 barcode solution was pipetted into to every second inlet (channel pattern: oligo, water, oligo, water, etc.) using a 20 µl pipette to achieve the desired alternating barcode pattern in the microwell rows. The system equilibrated for 30–40 min, with visual monitoring of the loading process. After loading, the vacuum layer was removed, and the system was resealed with q225 PCR film (non-sticky side, Quantagene, KUBO). The chip was centrifuged again at 3000 RPM for 2 min. Fluorescence intensity in both the 488-nm and 549-nm spectral channels was again measured across the microwell array.

Isolation of nuclei from the MCF-7 mammalian cell line

Nuclei were isolated using ATAC-RSB buffer which was prepared by mixing 500 µL of 1M Tris-HCl pH 7.4 (10 mM), 100 µL of 5M NaCl (10 mM), 150 µL of 1M MgCl2 (3 mM), and 49.25 mL of molecular biology grade water. The lysis buffer was prepared by adding 0.1% IGEPAL CA-630, 0.1% Tween-20, and 0.01% digitonin to ATAC-RSB buffer to reach the final volume. The wash buffer contained 0.1% Tween-20 in ATAC-RSB buffer.

One million viable MCF7 cells were transferred to 1.5 mL LoBind Eppendorf tubes and pelleted at 500 × g for 5 min at 4 °C. After discarding the supernatant, the pellet was rinsed in 1 mL ice-cold PBS, spun again under the same conditions, and the PBS removed. Cells were then lysed by adding 300 µL chilled lysis buffer, mixing gently, and incubating on ice for 5 min. Lysis was quenched with 1 mL cold wash buffer, followed by five gentle inversions. Nuclei were collected with a two-step spin - first with the hinges facing in, then facing out - both at 500 × g for 3 min at

4 °C. The supernatant was aspirated, and nuclei were resuspended in 250 µL of wash buffer. Nuclei were resuspended in 250 µL wash buffer using a wide-bore tip (Rainin) and counted on a Countess after mixing 1:1 with Trypan Blue. Then 50,000 nuclei were added to 1 ml of cold wash buffer and centrifuged first with the hinges facing in, then out - both at 500 × g for 5 min at 4 °C. The supernatant was removed and nuclei pellet was resuspended in 50 µl tagmentation cocktail prepared using 1× tagmentation buffer (Illumina Inc), 0.1% Tween 20, and 0.01% digitonin (Promega). TDE1 tagmentation enzyme (Tn5, Illumina Inc) was added to the cocktail at a ratio of 1:15. The tagmentation reaction was incubated at 37°C on a thermoshaker at 1000 RPM for 30 min. After tagmentation, 250 µL DNA binding buffer from Zymo DNA Clean and Concentrator Kit was added to the reaction, followed by clean up using the same kit. The concentration of tagmented DNA was measured by fluorimetry (Qubit).

PCR-on-chip

To prepare the chip for on-chip PCR and amplification, alternating rows of microwells were patterned with an solution-phase i5 index (via horizontal delivery layer) or an solution-phase i7 index (via vertical delivery layer). After barcoding, the microwell array layer was aligned with the PCR delivery layer and the vacuum layer was mated on top. The vacuum layer had four ports connected to the internal vacuum and one inlet for introducing PCR reagents. Next, the PCR master mix, composed of ultrapure water (Invitrogen), 1× NEB Master Mix (New England Biolabs), 0.005% Tween-20 (Promega), and BSA (1 mg/ml; Sigma-Aldrich) was prepared, and 8 µl of the master mix was combined with 2 µl of tagmented MCF7 DNA. Next, as previously described, the inlet was sealed with tape (600 Scotch Crystal, 3M), vacuum was applied for less <1 min, the inlet was opened, and the PCR mastermix with tagmented DNA (concentration: 0.454ng/ml) was introduced into the system. After confirming proper loading and stable applied vacuum, 20 µL of

mineral oil (Sigma Aldrich) was added, followed by an additional 50 μL of mineral oil on top of the inlet. Vacuum was released (the tubes were removed) and water was loaded into the vacuum layer using a syringe and all four ports to the vacuum. After that, all the ports were sealed with thermally conductive substrate polyimide film (Kapton Tape, thickness = 0.069 mm, 3M). Next, the microfluidic chip was placed in the Proflex PCR system (Life Technologies), covered with a coverslip, sealed, and subjected to 15 amplification cycles (98°C for 10 s, 63°C for 30 s, 72°C for 60 s) after an initial denaturation at 98°C for 30 s and gap filling at 72°C for 5 min.

DNA collection and cleanup

Post-PCR, the vacuum layer was carefully removed, and the layer and microwell array were cut and transferred to a petri dish. A series of washes to the delivery layer and microwell were performed using 2600 μL DNA Binding Buffer (Zymo Research), and the reagents were collected via a laboratory vacuum system. DNA was cleaned using Zymo DNA Clean and Concentrator Kit as instructed. Final elution was performed with 7 μL Elution Buffer (Zymo Research).

DNA quantification and quality control

DNA concentration was measured using the Qubit fluorometry system according to the manufacturer's instructions for the Qubit™ dsDNA HS Reagent (Invitrogen). DNA electropherograms were generated and assessed using a TapeStation (Agilent Technologies) with High Sensitivity D1000 Reagents.

Brightfield and fluorescence microscopy

Fluorescence intensity was measured using an Olympus IX51 microscope and filter sets for GFP and Texas Red equipped with ImageJ (NIH, USA) imaging software.

Results

Barcoding principle and design of deterministic loading process

To design a bead-free barcoding approach suitable for NGS from a 512 microwell array (Figure 1A,B), we designed a barcoding strategy with two aspects: (1) a CDI scheme is employed for barcode design using Illumina i5 and i7 indexes and (2) a deterministic barcode loading scheme fluidically delivers solution-phase unique barcode combinations to each of the 512 microwells in the planar microwell array. The barcode scheme is designed for endpoint Illumina sequencing of pooled barcoded DNA samples, with an interest here in the intermediate steps of on-chip PCR followed by DNA quality control by Tapestation analysis (Figure 1C). Adoption of a bead-free, aqueous barcoding strategy requires low-crosstalk delivery of unique barcodes to each of the 512 microwells. Informed by the work of Hu et al.[22] we designed a vacuum-driven microfluidic system based on a grid-patterning approach inspired by DBiT-Seq[18]. To uniquely barcode each microwell, we used a multi-step, vacuum-assisted loading process. Unlike other approaches[29,30], fluid flow was driven by house vacuum via pressure differences across the microwell, delivery, and vacuum layers.[31] The first barcode set was delivered via the horizontal delivery network (i5) and then a second set via the vertical delivery network (i7), creating a CDI scheme.

This approach produces 512 microwells, each with a unique barcode combination. The microwell, delivery, and vacuum layers were manually aligned under a stereomicroscope, sealed, and connected to house vacuum (45-60 s). Evacuation through the PDMS layer created a pressure gradient (Figure 1D), confirmed by microwell perimeter bowing. After releasing the vacuum, barcode solutions (0.3-0.7 µm per channel) were pipetted into inlets, flowing by suction through bifurcated microchannels to fill dead-end microwells. Air was introduced to clear excess solution

and cap each microwell, enabling deterministic barcoding and subsequent on-chip PCR. The process followed two steps: first, the vertical network delivered i5 solutions, which evaporated to leave residues in the patterned microwells; next, the vertical layer was removed and replaced with a perpendicular horizontal network for i7 delivery. After a second loading, each microwell contained a unique i5/i7 pair

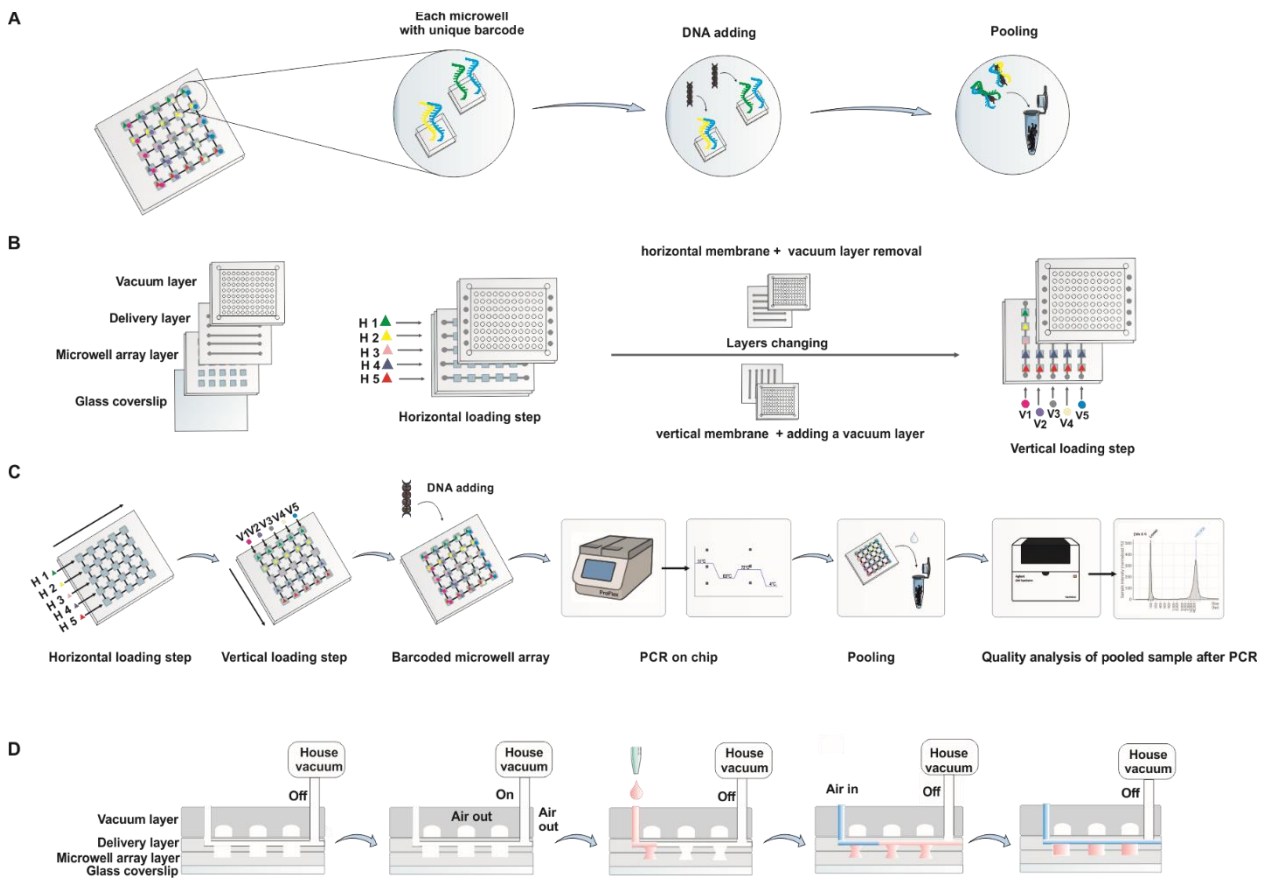

Figure 1. Deterministic, bead-free oligonucleotide barcoding of arrayed microwells using a multi-layer vacuum-driven microfluidic network. (A) Use of aqueous barcodes and deterministic loading of unique barcodes to each microwell in the array allows pooling of barcoded samples for downstream analysis (e.g., sequencing). (B) Diagram of the barcoding system. The process includes sequential horizontal and vertical loading stages, with drying and layer exchange between

the steps to ensure deterministic assignment of barcodes. (C) To achieve 512 uniquely barcoded microwells, the workflow includes a two-step aqueous barcode loading process (horizontal and the vertical delivery of barcodes), sample (e.g., DNA) loading, on-chip PCR, collection and pooling of barcoded samples for pooled analysis of DNA quality by electrophoresis (Tapestation). (D) A multi-layer PDMS microdevice is designed to pattern unique aqueous barcodes into each of an array of dead-end microwells using the gas permeability of PDMS and applied suction to drive the flow of reagents to each microwell.

Microfluidic device designs for deterministic barcoding process

The vacuum-assisted microfluidic system consists of three PDMS layers: a microwell array layer, a set of three interchangeable fluid delivery layers (Figure 2 A) (used sequentially for horizontal barcode loading, vertical barcode loading, and PCR reagent delivery), and a vacuum layer. The microwell array layer contains only microwells (512 in total, 32 × 16) without channels, while the fluidic networks, inlets, and narrow necks (90 µm × 150 µm) are fully integrated into the 100 µm-thick delivery layers. The narrow neck functions as a microfluidic constriction that reduces or prevents backflow from the microwell into the main channel[32,33], thereby reducing the risk of cross-contamination between adjacent microwells (Figure 2 B).

Each microwell in the microwell array layer measures 250 × 350 × 100 µm, with horizontal and vertical pitches of 550 µm and 450 µm to reduce the risk of cross-contamination. When mated to the fluid delivery layers, the assembly extends the effective microwell depth to 200 µm. Each microchannel has a separate inlet to confine the introduction of barcode solutions uniquely to that microchannel and the associated row of microwells.[22] Unlike bead-based barcoding systems, the

aqueous barcoding strategy using fluid filling and not external magnetic forces (e.g., as used with the more common oligo-conjugated magnetic beads) to retain barcodes inside microwells after loading (Figure 2 C), making the constriction design critical for robust operation.[10,34]

During the horizontal loading step, i5 barcodes are delivered through 16 parallel channels (45 mm × 150 µm × 100 µm) with 1.5 mm inlets. The vertical delivery layer introduces i7 barcodes via 32 perpendicular channels (34 mm × 200 µm × 100 µm), each with a dead-end design, allowing deterministic CDI while minimizing uncontrolled flow. The vacuum layer (~7 mm thick) contains four ports for facile connection to the house vacuum system via Tygon tubing (∅ = 0.02 inches). The central region of this layer is comprised an array of 200 µm cylindrical micropillars, designed to evenly distribute suction force and ensure stable attachment when mated to the delivery layer. The vacuum layer featured 16 open inlets for horizontal delivery and 32 for vertical delivery, matching the number of microchannels used for each barcode set. As mentioned, the deterministic loading approach was adaptable to reagent delivery for on-chip PCR. When used for PCR, a PCR reagent-delivery layer was used and contained both an integrated network of microchannels and a microwell array matched to that of the microwell array layer. The PCR layer was designed with a single inlet for uniform and simultaneous delivery of all PCR reaction reagents, and minimizing reagent loss.

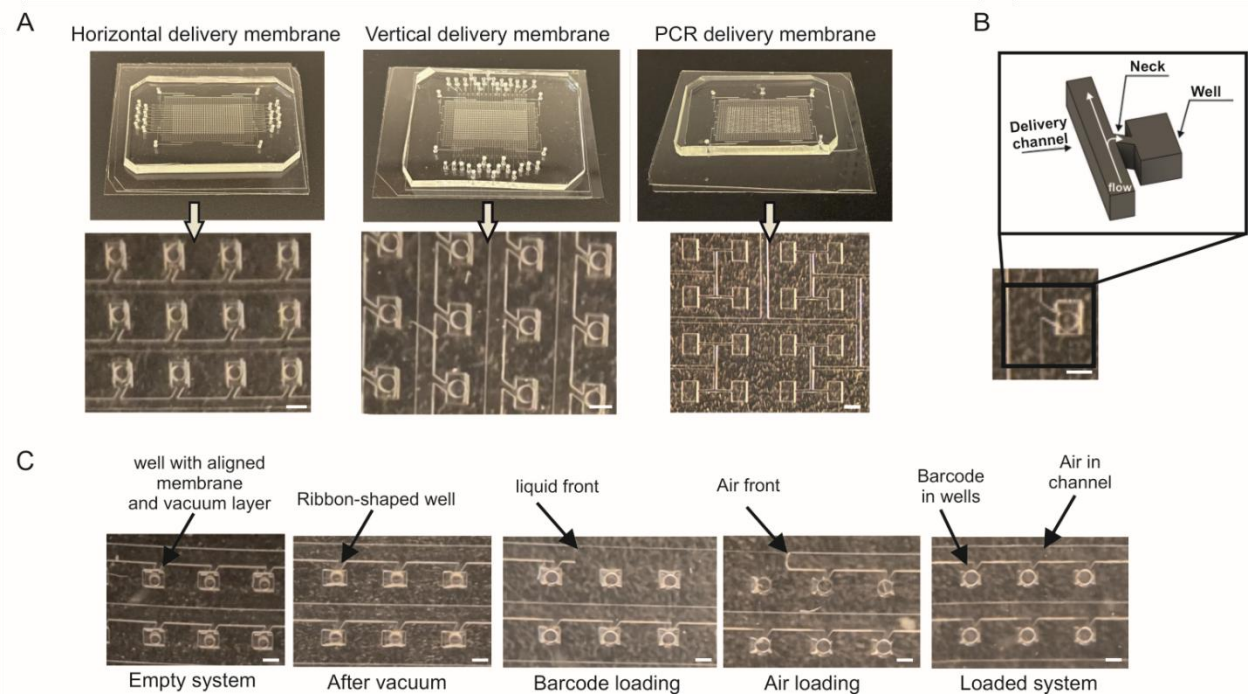

Figure 2. Microfluidic networks are designed to pattern specific microwells with aqueous oligonucleotide barcode solutions. (A) Brightfield images and close-up views show three different device configurations, each is seated on the microwell array layer and a glass slide: a horizontal delivery layer, a vertical delivery layer, and a PCR-reagent delivery layer. (B) Bright field micrograph and schematic representative of the interface between the main delivery microchannel and a necked microwell. (C) Brightfield micrographs show the sequential stages of barcode-solution loading using the delivery layers to fill each microwell. Scale bars: 250 µm.

Patterning of aqueous barcodes using the deterministic barcoding technique

To assess the capacity for scale up, we sought to understand the relevant time scales for each step. First, we look at the set up. Once assembled, there are a series of steps that include the barcode loading time, including (i) placement of aliquots on inlets (approx. 1 minute), (ii) flow into microchannels (approx. 15-20 minutes), and (iii) fill of microchannels with air (approx. 20

minutes). Next, we considered the time it takes to remove the first delivery layer and attach the second delivery layer, including alignment (approx. 10 minutes). We also considered the loading uniformity. To assess the loading uniformity of the barcode solutions for all microwells, solutions of fluorescently labeled oligonucleotide (biotin-i51-488 and oligo-A549) were introduced into the microsystem (Figure 3 D), and the coefficient of variation (CV) of fluorescence intensity in the microwells was analyzed as a measure of filling uniformity. In the horizontal loading step (Figure 3 A, B, C), the CV of the fluorescence intensity was inversely related to the loading volume (V = 0.4 μL, CV = 37%; V = 0.5 μL, CV = 29%; V = 0.6 μL, CV = 20%) until the loaded volume of 0.7 μL (CV = 24%). The slight rise in CV from 0.6 to 0.7 μL suggests microwell overfilling. The analysis indicates 0.6 μL is an optimal loading volume for this device and loading protocol design.

In the vertical loading step (Figure 3 E, F, G), a similar analysis suggests the CV in microwell-to-microwell fluorescence intensity is minimized by loading a volume of 0.5 μL, with lower overall CV values for the volumes analyzed (V = 0.3 μL, CV = 21%; V = 0.4 μL, CV = 13%; V = 0.5 μL, CV = 17%; V = 0.6 μL, CV = 10%;) (Figure 3 D, E). The lower CVs for the vertical loading step versus the horizontal loading step are attributed to the lower number of microwells connected to each distribution microchannel in the vertical configuration, which likely minimizes flow resistance variability and enhances control of fluid flow. Importantly, benchmarking of the microwell loading variability of this system against similar vacuum-assisted delivery techniques[22,33,35,36] developed for other reagent-delivery purposes is favorable.

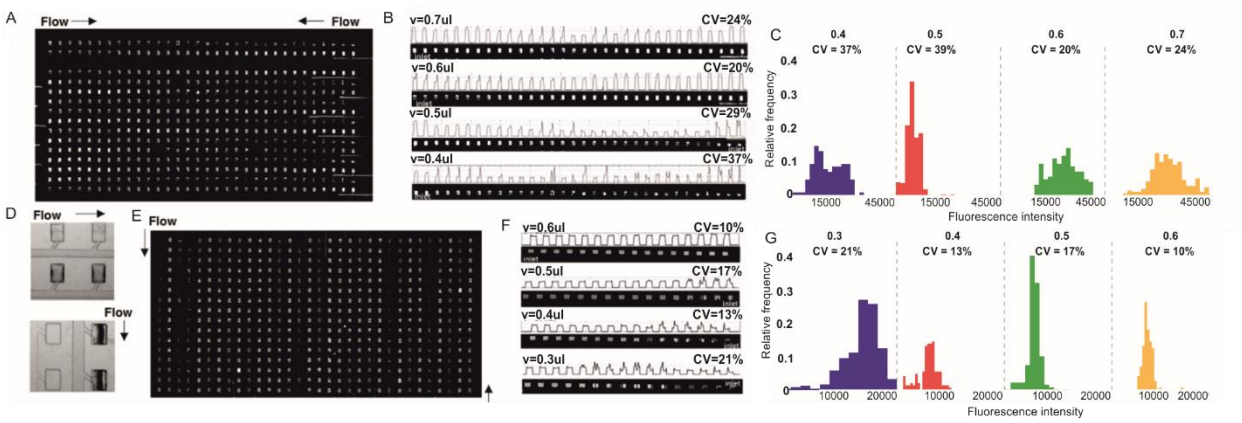

Figure 3. Vacuum-assisted loading of oligonucleotide solutions to the microwell array. (A) Fluorescence micrograph reporting endpoint fluorescence signal from the horizontal loading step of the aqueous barcoding workflow. Arrows who the direction of flow. (B, C) Fluorescence intensity profiles and histograms for different volumes of barcode solution loaded through the horizontal delivery layer, highlighting differences in microwell filling efficiency depending on the volume. (D) Brightfield micrographs depicting flow microchannels and microwell structures, where dark microwells indicate filled microwells and bright microwells remain empty. (E) Fluorescence micrograph reporting endpoint fluorescence signal from the vertical loading step of the aqueous barcoding workflow. Arrows who the direction of flow. (F, G) Fluorescence intensity profiles and histograms for different volumes of barcode solution loaded through the vertical delivery layer, highlighting differences in microwell filling efficiency depending on the volume.

Cross-contamination of the deterministic barcoding technique

To evaluate the potential for cross-contamination between adjacent microwells, we scrutinized both the horizontal and vertical loading steps by imaging fluorescently labeled oligonucleotide probe signal. First, to understand cross-contamination associated with the horizontal delivery layer, we used the vacuum-assisted system to introduce a fluorescent barcode solution (oligo-

A549) into every second microchannel, while concurrently filling interdigitated microchannels with a non-fluorescing solution (DI water). Fluorescence micrographs (Figure 4A) show negligible fluorescence signal in the rows of water-filled microwells, after the horizontal delivery was completed. To the same microwell array, we used a vertical delivery layer to introduce a second barcode (biotin-i51-488), which fluoresces in a different spectral channel.

Here, we observed one failure mode. The fluorescence micrographs in Figure 4B (top) show water-filled microwells that exhibit detectable oligo-A549 fluorescence signal, thus indicating cross-contamination introduced when swapping out the horizontal delivery layer for the vertical delivery layer. For comparison, Figure 4B (bottom) shows other microwells on the same array with no detectable cross-contamination.

Encompassing the footprint of the entire chip, Figure 4C is a heat map of fluorescence intensity from aqueous barcodes (488-nm channel) delivered by the horizontal delivery layer after completion of the two-stage barcoding workflow using the vacuum-assisted deterministic barcoding device. While detecting fluorescence signal in the horizontal barcode rows (H1-H16), we observed detectable fluorescence signal in 20 of microwells from the water-filled (W) rows, indicating ~4.0% cross-contamination, which compares favorably to 5-10% cross-contamination for previous methods.[37–39]

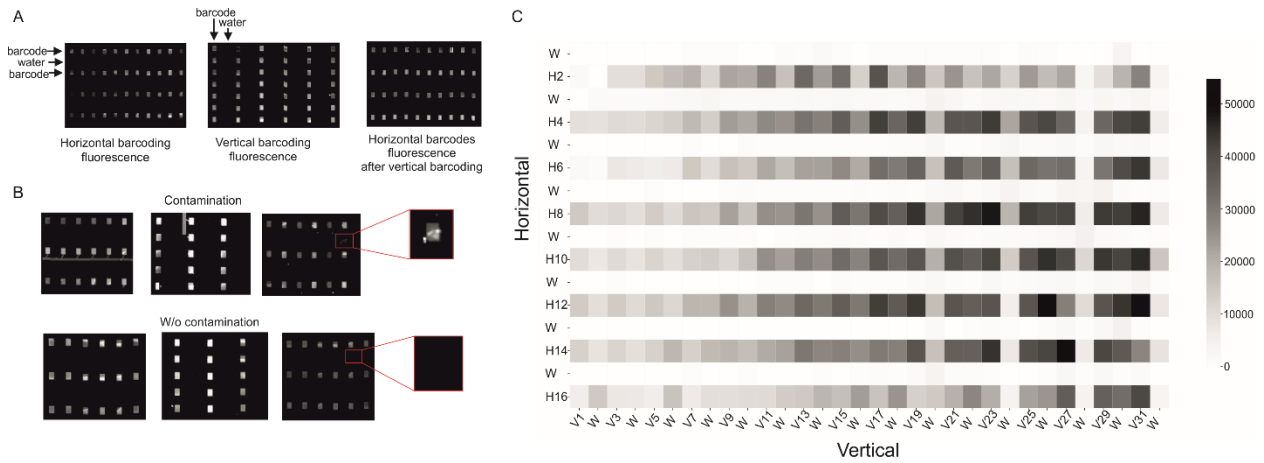

Figure 4. Validation of the vacuum-driven microwell barcoding system. (A) Fluorescence micrographs showing horizontal barcoding, vertical barcoding, and the resulting horizontal barcode fluorescence after vertical barcoding. (B) Representative images demonstrating the effect of contamination (top) and the absence of contamination (bottom), with insets highlighting individual microwells. Contamination (barcode transfer between adjacent microwells) can occur during layer changes (from horizontal to vertical). Contaminated microwells are marked as shown in the top panel. (C) Heatmap of fluorescence intensities corresponding to horizontal (H1–H16) and vertical (V1–V32) barcodes. In this configuration, every second row and column contained either barcode solution or water (e.g., H1 – water, H2 – barcode, H3 – water). High fluorescence intensities observed in rows or columns corresponding to water indicate contamination in those microwells.

PCR-on-chip

To evaluate the performance of the deterministic barcoding strategy, we applied it to load i5 and i7 indexes into microwells for the amplification of labeled DNA, serving as the final step prior to

ATAC-seq library preparation (Figure 5 A). This process was carried out following the protocol detailed in the Experimental section (PCR-on-chip). Labeling of MCF-7 nuclei with Tn5 produced an initial library concentration of 0.454 ng/µl. Subsequently, the Index-PCR master mix containing the labeled DNA was added to each microwell preloaded with dried barcodes (i5, i7). On-chip amplification for 15 cycles increased the library concentration ~12-fold to 5.6 ng/µl, confirming efficient PCR and successful incorporation of the dual indexes across all microwells. Tapestation electropherograms (Figure 5 B) displayed the characteristic tri-modal size distribution of high-quality ATAC-seq libraries, with prominent peaks at ~200 bp (nucleosome-free regions), ~350 bp (mononucleosomes), and ~550 bp (dinucleosomes). The absence of adapter dimers and the clear separation between peaks indicate high library complexity and minimal over-amplification, validating the suitability of the preparation for downstream pooling and high-depth sequencing.

The microwell-based deterministic indexing strategy offers several advantages over conventional tube-based workflows or previously reported microwell-based methods.[5,10,21,40] First, pre-loading dried i5/i7 primers eliminates liquid-handling steps that can introduce cross-contamination, thereby maintaining single-sample integrity throughout amplification. Second, the confined reaction volumes (<200 nL) enhance primer-template hybridization kinetics, reducing the number of PCR cycles required to reach sequencing-ready concentrations.

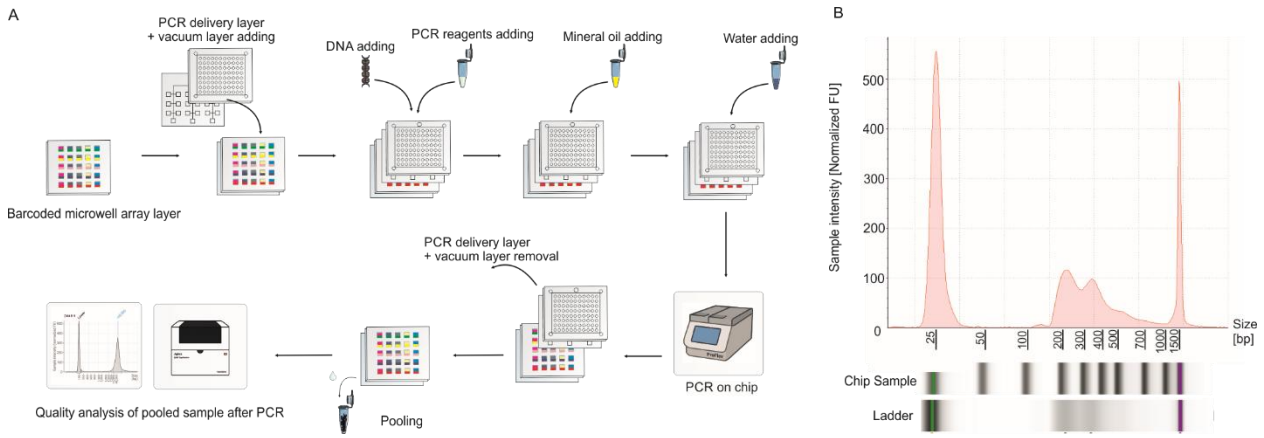

Figure 5. Workflow and validation of on-chip PCR using barcoded microwell arrays. (A) Schematic overview of the PCR-on-chip process. The encoded microwell array was combined with PCR and vacuum layers, enabling compartmentalized amplification after sequential addition of DNA and reagents. Pooled samples were then collected for analysis. (B) TapeStation analysis of pooled barcoded DNA samples, confirming barcode integrity and fragment size distribution.

Conclusions

Barcoding strategies described in the literature are largely based on oligonucleotide-coated magnetic particles, typically delivered by peristaltic pumps.[1,41,42] In contrast, we developed a multi-layer PDMS system in which fluid flow is driven exclusively by a standard laboratory vacuum (house vacuum), which eliminates the need for external pumps, simplifying system integration and making the platform accessible to laboratories without specialized fluidic equipment. Our platform delivers barcodes as free oligonucleotides, eliminating the need for time-consuming synthesis, preparation, and purification steps required for beads. This approach

eliminates issues related to uneven bead distribution and incomplete microwell filling, while also minimizing the risk of mechanical contamination and carryover from bead surfaces.

The device features a 512-well layer, thin PDMS delivery layers, and a vacuum-connected suction layer that drives continuous liquid flow, enabling efficient delivery of 512 barcodes and precise sample labeling. We validated the system using fluorescein and fluorophore-labeled oligonucleotides to ensure uniform loading, optimize reagent use, and assess cross-contamination risk, confirming high selectivity and reliability. Deterministic assignment of i5 and i7 indexes for DNA amplification demonstrated the generation of high-quality, dual-indexed ATAC-seq libraries.

Our platform combines the strengths of existing high-throughput systems while minimizing contamination, reagent use, and library preparation time. Optimized on-chip PCR prevents leakage and material loss. Its intuitive design allows easy integration into standard laboratories, offering a flexible and scalable solution for high-throughput genomic analyses, including dual-indexed ATAC-seq.

Acknowledgement

Funding for this work was provided by the US National Institutes of Health (R01CA20301, A.E.H.) and the Chan Zuckerberg Biohub San Francisco Investigator Award (A.E.H.). We express sincere gratitude to the Kosciuszko Foundation for the generous support provided through the Exchange to the US Fellowship during the 2024/2025 academic year, which significantly

contributed to the successful completion of this research and enhanced ties between our two nations, Poland and the US.

References:

(1) Macosko, E. Z.; Basu, A.; Satija, R.; Nemesh, J.; Shekhar, K.; Goldman, M.; Tirosh, I.; Bialas, A. R.; Kamitaki, N.; Martersteck, E. M.; Trombetta, J. J.; Weitz, D. A.; Sanes, J. R.; Shalek, A. K.; Regev, A.; McCarroll, S. A. Highly Parallel Genome-Wide Expression Profiling of Individual Cells Using Nanoliter Droplets. *Cell* **2015**, *161* (5), 1202–1214. https://doi.org/10.1016/j.cell.2015.05.002.

(2) Aynaud, M.-M.; Hernandez, J. J.; Barutcu, S.; Braunschweig, U.; Chan, K.; Pearson, J. D.; Trcka, D.; Prosser, S. L.; Kim, J.; Barrios-Rodiles, M.; Jen, M.; Song, S.; Shen, J.; Bruce, C.; Hazlett, B.; Poutanen, S.; Attisano, L.; Bremner, R.; Blencowe, B. J.; Mazzulli, T.; Han, H.; Pelletier, L.; Wrana, J. L. A Multiplexed, next Generation Sequencing Platform for High-Throughput Detection of SARS-CoV-2. *Nat. Commun.* **2021**, *12* (1), 1405. https://doi.org/10.1038/s41467-021-21653-y.

(3) Gostel, M. R.; Kress, W. J. The Expanding Role of DNA Barcodes: Indispensable Tools for Ecology, Evolution, and Conservation. *Diversity* **2022**, *14* (3), 213. https://doi.org/10.3390/d14030213.

(4) Kim, S. C.; Haliburton, J. R.; Gartner, Z. J.; Abate, A. R. Single-Cell Protein Profiling by Microdroplet Barcoding and Next-Generation Sequencing. *Methods Mol. Biol. Clifton NJ* **2022**, *2386*, 101–111. https://doi.org/10.1007/978-1-0716-1771-7_7.

(5) Lin, S.; Yin, K.; Zhang, Y.; Lin, F.; Chen, X.; Zeng, X.; Guo, X.; Zhang, H.; Song, J.; Yang, C. Well-TEMP-Seq as a Microwell-Based Strategy for Massively Parallel Profiling of Single-Cell Temporal RNA Dynamics. *Nat. Commun.* **2023**, *14* (1), 1272. https://doi.org/10.1038/s41467-023-36902-5.

(6) Yang, L.; Wang, Z.; Deng, Y.; Li, Y.; Wei, W.; Shi, Q. Single-Cell, Multiplexed Protein Detection of Rare Tumor Cells Based on a Beads-on-Barcode Antibody Microarray. *Anal. Chem.* **2016**, *88* (22), 11077–11083. https://doi.org/10.1021/acs.analchem.6b03086.

(7) Danielski, K. Guidance on Processing the 10x Genomics Single Cell Gene Expression Assay. *Methods Mol. Biol. Clifton NJ* **2023**, *2584*, 1–28. https://doi.org/10.1007/978-1-0716-2756-3_1.

(8) Juzenas, S.; Goda, K.; Kiseliovas, V.; Zvirblyte, J.; Quintinal-Villalonga, A.; Siurkus, J.; Nainys, J.; Mazutis, L. inDrops-2: A Flexible, Versatile and Cost-Efficient Droplet Microfluidic Approach for High-Throughput scRNA-Seq of Fresh and Preserved Clinical Samples. *Nucleic Acids Res.* **2025**, *53* (2), gkae1312. https://doi.org/10.1093/nar/gkae1312.

(9) Picelli, S.; Björklund, Å. K.; Faridani, O. R.; Sagasser, S.; Winberg, G.; Sandberg, R. Smart-Seq2 for Sensitive Full-Length Transcriptome Profiling in Single Cells. *Nat. Methods* **2013**, *10* (11), 1096–1098. https://doi.org/10.1038/nmeth.2639.

(10) Gierahn, T. M.; Wadsworth, M. H.; Hughes, T. K.; Bryson, B. D.; Butler, A.; Satija, R.; Fortune, S.; Love, J. C.; Shalek, A. K. Seq-Well: A Portable, Low-Cost Platform for High-Throughput Single-Cell RNA-Seq of Low-Input Samples. *Nat. Methods* **2017**, *14* (4), 395–398. https://doi.org/10.1038/nmeth.4179.

(11) Martin, B. K.; Qiu, C.; Nichols, E.; Phung, M.; Green-Gladden, R.; Srivatsan, S.; Blecher-Gonen, R.; Beliveau, B. J.; Trapnell, C.; Cao, J.; Shendure, J. Optimized Single Nucleus Transcriptional Profiling by Combinatorial Indexing. *Nat. Protoc.* **2023**, *18* (1), 188–207. https://doi.org/10.1038/s41596-022-00752-0.
(12) Chen, Y.; Song, J.; Ruan, Q.; Zeng, X.; Wu, L.; Cai, L.; Wang, X.; Yang, C. Single-Cell Sequencing Methodologies: From Transcriptome to Multi-Dimensional Measurement. *Small Methods* **2021**, *5* (6), 2100111. https://doi.org/10.1002/smtd.202100111.
(13) Lareau, C. A.; Ma, S.; Duarte, F. M.; Buenrostro, J. D. Inference and Effects of Barcode Multiplets in Droplet-Based Single-Cell Assays. *Nat. Commun.* **2020**, *11* (1), 866. https://doi.org/10.1038/s41467-020-14667-5.
(14) Lun, A. T. L.; Riesenfeld, S.; Andrews, T.; Dao, T. P.; Gomes, T.; participants in the 1st Human Cell Atlas Jamboree; Marioni, J. C. EmptyDrops: Distinguishing Cells from Empty Droplets in Droplet-Based Single-Cell RNA Sequencing Data. *Genome Biol.* **2019**, *20* (1), 63. https://doi.org/10.1186/s13059-019-1662-y.
(15) Thielecke, L.; Aranyossy, T.; Dahl, A.; Tiwari, R.; Roeder, I.; Geiger, H.; Fehse, B.; Glauche, I.; Cornils, K. Limitations and Challenges of Genetic Barcode Quantification. *Sci. Rep.* **2017**, *7*, 43249. https://doi.org/10.1038/srep43249.
(16) Leng, Y.; Sun, K.; Chen, X.; Li, W. Suspension Arrays Based on Nanoparticle-Encoded Microspheres for High-Throughput Multiplexed Detection. *Chem. Soc. Rev.* **2015**, *44* (15), 5552–5595. https://doi.org/10.1039/c4cs00382a.
(17) Kuijpers, L.; Hornung, B.; van den Hout - van Vroonhoven, M. C. G. N.; van IJcken, W. F. J.; Grosveld, F.; Mulugeta, E. Split Pool Ligation-Based Single-Cell Transcriptome Sequencing (SPLiT-Seq) Data Processing Pipeline Comparison. *BMC Genomics* **2024**, *25* (1), 361. https://doi.org/10.1186/s12864-024-10285-3.
(18) Liu, Y.; Yang, M.; Deng, Y.; Su, G.; Enninful, A.; Guo, C. C.; Tebaldi, T.; Zhang, D.; Kim, D.; Bai, Z.; Norris, E.; Pan, A.; Li, J.; Xiao, Y.; Halene, S.; Fan, R. High-Spatial-Resolution Multi-Omics Sequencing via Deterministic Barcoding in Tissue. *Cell* **2020**, *183* (6), 1665-1681.e18. https://doi.org/10.1016/j.cell.2020.10.026.
(19) Rowe, C. A.; Scruggs, S. B.; Feldstein, M. J.; Golden, J. P.; Ligler, F. S. An Array Immunosensor for Simultaneous Detection of Clinical Analytes. *Anal. Chem.* **1999**, *71* (2), 433–439. https://doi.org/10.1021/ac980798t.
(20) Wirth, J.; Huber, N.; Yin, K.; Brood, S.; Chang, S.; Martinez-Jimenez, C. P.; Meier, M. Spatial Transcriptomics Using Multiplexed Deterministic Barcoding in Tissue. *Nat. Commun.* **2023**, *14*, 1523. https://doi.org/10.1038/s41467-023-37111-w.
(21) Shi, W.; Zhang, J.; Huang, S.; Fan, Q.; Cao, J.; Zeng, J.; Wu, L.; Yang, C. Next-Generation Sequencing-Based Spatial Transcriptomics: A Perspective from Barcoding Chemistry. *JACS Au* **2024**, *4* (5), 1723–1743. https://doi.org/10.1021/jacsau.4c00118.
(22) Hu, J.; Chen, L.; Zhang, P.; Hsieh, K.; Li, H.; Yang, S.; Wang, T.-H. A Vacuum-Assisted, Highly Parallelized Microfluidic Array for Performing Multi-Step Digital Assays. *Lab. Chip* **2021**, *21* (23), 4716–4724. https://doi.org/10.1039/D1LC00636C.
(23) Witek, M. A.; Hupert, M. L.; Park, D. S.-W.; Fears, K.; Murphy, M. C.; Soper, S. A. 96-Well Polycarbonate-Based Microfluidic Titer Plate for High-Throughput Purification of DNA and RNA. *Anal. Chem.* **2008**, *80* (9), 3483–3491. https://doi.org/10.1021/ac8002352.
(24) Zhou, W.; Yan, Y.; Guo, Q.; Ji, H.; Wang, H.; Xu, T.; Makabel, B.; Pilarsky, C.; He, G.; Yu, X.; Zhang, J. Microfluidics Applications for High-Throughput Single Cell Sequencing. *J. Nanobiotechnology* **2021**, *19* (1), 312. https://doi.org/10.1186/s12951-021-01045-6.

(25) Chen, T. N.; Gupta, A.; Zalavadia, M.; Streets, A. M. μCB-Seq: Microfluidic Cell Barcoding and Sequencing for High-Resolution Imaging and Sequencing of Single Cells. *Lab. Chip* **2020**, *20* (21), 3899–3913. https://doi.org/10.1039/d0lc00169d.
(26) Xie, Y.; Chen, Z.; Cai, D.; Huang, D.; Huang, E.; Yang, X.; Zhang, T.; Wen, H.; Wang, Y.; Zhao, M.; Liu, D.; Xu, B. Rapid Detection of Uropathogens Using an Integrated Multiplex Digital Nucleic Acid Detection Assay Powered by a Digital-to-Droplet Microfluidic Device. *Anal. Chem.* **2024**, *96* (30), 12561–12569. https://doi.org/10.1021/acs.analchem.4c02578.
(27) Kantak, M.; Batra, P.; Shende, P. Integration of DNA Barcoding and Nanotechnology in Drug Delivery. *Int. J. Biol. Macromol.* **2023**, *230*, 123262. https://doi.org/10.1016/j.ijbiomac.2023.123262.
(28) Meyer, M.; Kircher, M. Illumina Sequencing Library Preparation for Highly Multiplexed Target Capture and Sequencing. *Cold Spring Harb. Protoc.* **2010**, *2010* (6), pdb.prot5448. https://doi.org/10.1101/pdb.prot5448.
(29) Wang, A.; Koh, D.; Schneider, P.; Breloff, E.; Oh, K. W. A Compact, Syringe-Assisted, Vacuum-Driven Micropumping Device. *Micromachines* **2019**, *10* (8), 543. https://doi.org/10.3390/mi10080543.
(30) Sarma, M.; Lee, J.; Ma, S.; Li, S.; Lu, C. A Diffusion-Based Microfluidic Device for Single-Cell RNA-Seq. *Lab. Chip* **2019**, *19* (7), 1247–1256. https://doi.org/10.1039/c8lc00967h.
(31) Xu, L.; Lee, H.; Jetta, D.; Oh, K. W. Vacuum-Driven Power-Free Microfluidics Utilizing the Gas Solubility or Permeability of Polydimethylsiloxane (PDMS). *Lab. Chip* **2015**, *15* (20), 3962–3979. https://doi.org/10.1039/C5LC00716J.
(32) Azizian, P.; Casals-Terré, J.; Ricart, J.; M. Cabot, J. Capillary-Driven Microfluidics: Impacts of 3D Manufacturing on Bioanalytical Devices. *Analyst* **2023**, *148* (12), 2657–2675. https://doi.org/10.1039/D3AN00115F.
(33) Kolnik, M.; Tsimring, L. S.; Hasty, J. Vacuum-Assisted Cell Loading Enables Shear-Free Mammalian Microfluidic Culture. *Lab. Chip* **2012**, *12* (22), 4732–4737. https://doi.org/10.1039/c2lc40569e.
(34) Lammertse, E.; Li, S.; Kendall, J.; Kim, C.; Morris, P.; Ranade, N.; Levy, D.; Wigler, M.; Brouzes, E. Magnetically Functionalized Hydrogels for High-Throughput Genomic Applications. *Adv. Mater. Technol.* **2024**, *9* (2), 2301155. https://doi.org/10.1002/admt.202301155.
(35) Liang, D. Y.; Tentori, A. M.; Dimov, I. K.; Lee, L. P. Systematic Characterization of Degas-Driven Flow for Poly(Dimethylsiloxane) Microfluidic Devices. *Biomicrofluidics* **2011**, *5* (2), 024108. https://doi.org/10.1063/1.3584003.
(36) Gao, Y.; Li, P.; Pappas, D. A Microfluidic Localized, Multiple Cell Culture Array Using Vacuum Actuated Cell Seeding: Integrated Anticancer Drug Testing. *Biomed. Microdevices* **2013**, *15* (6), 10.1007/s10544-013-9779–3. https://doi.org/10.1007/s10544-013-9779-3.
(37) Larsson, A. J. M.; Stanley, G.; Sinha, R.; Weissman, I. L.; Sandberg, R. Computational Correction of Index Switching in Multiplexed Sequencing Libraries. *Nat. Methods* **2018**, *15* (5), 305–307. https://doi.org/10.1038/nmeth.4666.
(38) Bach, K.; Pensa, S.; Grzelak, M.; Hadfield, J.; Adams, D. J.; Marioni, J. C.; Khaled, W. T. Differentiation Dynamics of Mammary Epithelial Cells Revealed by Single-Cell RNA Sequencing. *Nat. Commun.* **2017**, *8* (1), 2128. https://doi.org/10.1038/s41467-017-02001-5.
(39) Li, T.; Alvarez, M.; Liu, C.; Abuhanna, K.; Sun, Y.; Ernst, J.; Plath, K.; Balliu, B.; Luo, C.; Zaitlen, N. The Impact of Ambient Contamination on Demultiplexing Methods for Single-Nucleus Multiome Experiments. *eLife* **2025**, *14*. https://doi.org/10.7554/eLife.106769.1.

(40) Bai, R.; Li, L.; Liu, M.; Yan, S.; Miao, C.; Li, R.; Luo, Y.; Liu, T.; Lin, B.; Ji, Y.; Lu, Y. Paper-Based 3D Scaffold for Multiplexed Single Cell Secretomic Analysis. *Anal. Chem.* **2018**, *90* (9), 5825–5832. https://doi.org/10.1021/acs.analchem.8b00362.
(41) Berneman, N.; Jimidar, I.; Van Geite, W.; Gardeniers, H.; Desmet, G. Rapid Vacuum-Driven Monolayer Assembly of Microparticles on the Surface of Perforated Microfluidic Devices. *Powder Technol.* **2021**, *390*, 330–338. https://doi.org/10.1016/j.powtec.2021.05.079.
(42) Delley, C. L.; Abate, A. R. Modular Barcode Beads for Microfluidic Single Cell Genomics. *Sci. Rep.* **2021**, *11* (1), 10857. https://doi.org/10.1038/s41598-021-90255-x.

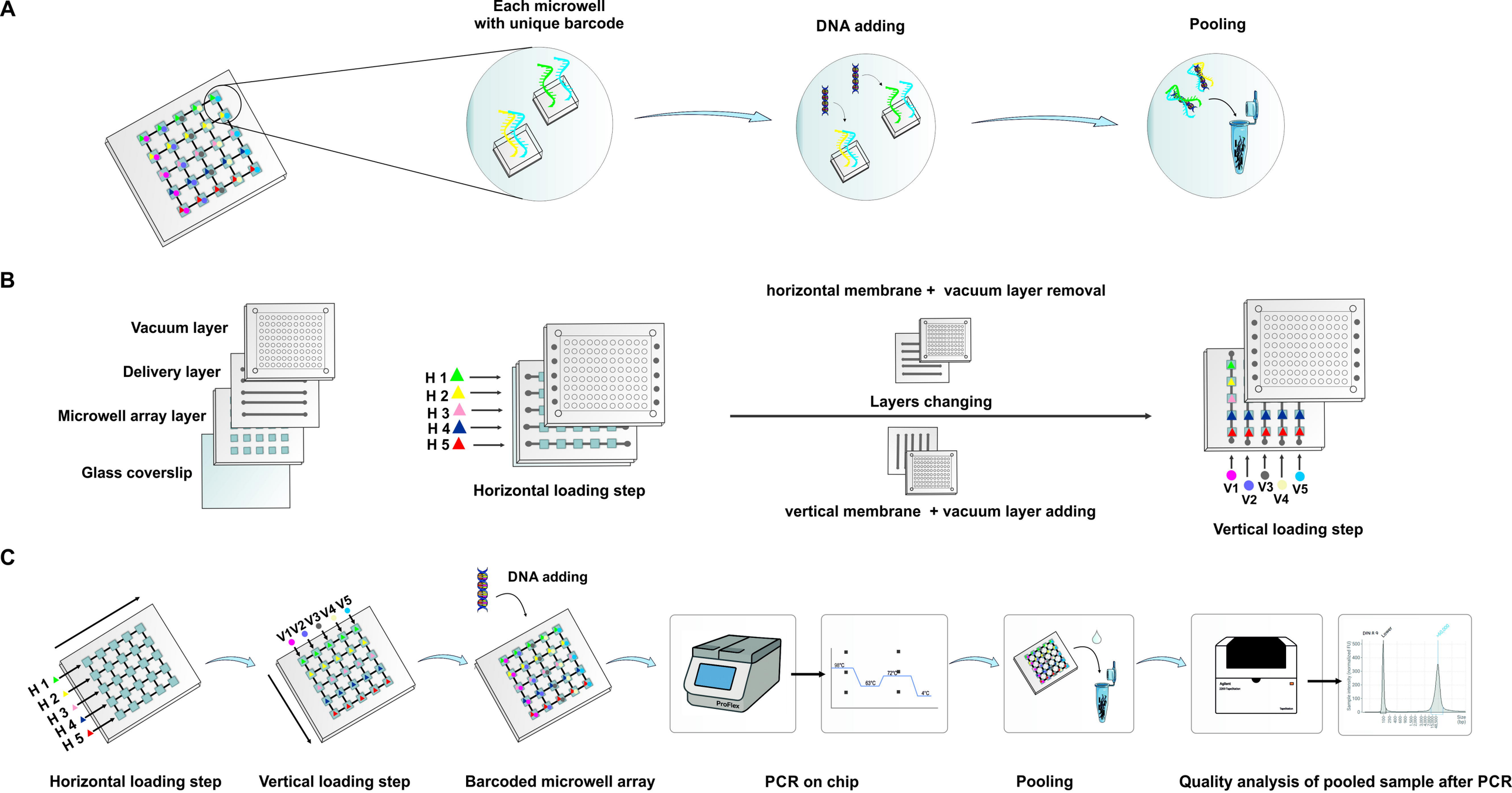
A
Each microwell
with unique barcode
DNA adding
Pooling
B
Vacuum layer
Delivery layer
Microwell array layer
Glass coverslip
H 1
H 2
H 3
H 4
H 5
Horizontal loading step
horizontal membrane + vacuum layer removal
Layers changing
vertical membrane + vacuum layer adding
V1
V2
V3
V4
V5
Vertical loading step
C
H 1
H 2
H 3
H 4
H 5
V1V2V3V4V5
DNA adding
ProFlex
98°C
63°C
72°C
4°C
Horizontal loading step
Vertical loading step
Barcoded microwell array
PCR on chip
Pooling
Quality analysis of pooled sample after PCR
D
House
vacuum
Off
On
Air out
Air
out
Air in
Vacuum layer
Delivery layer
Microwell array layer
Glass coverslip

A

Horizontal delivery membrane

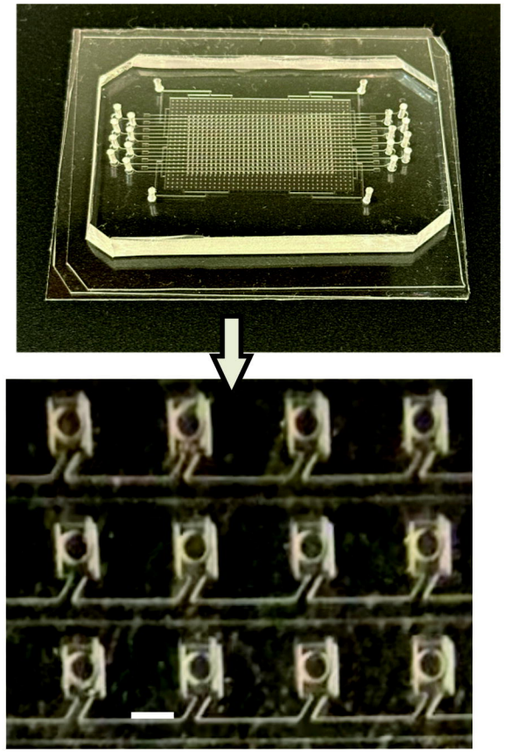

Vertical delivery membrane

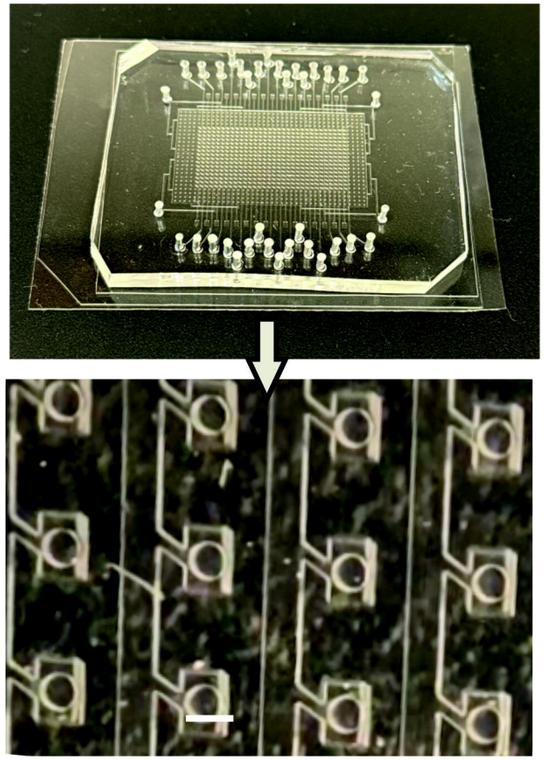

PCR delivery membrane

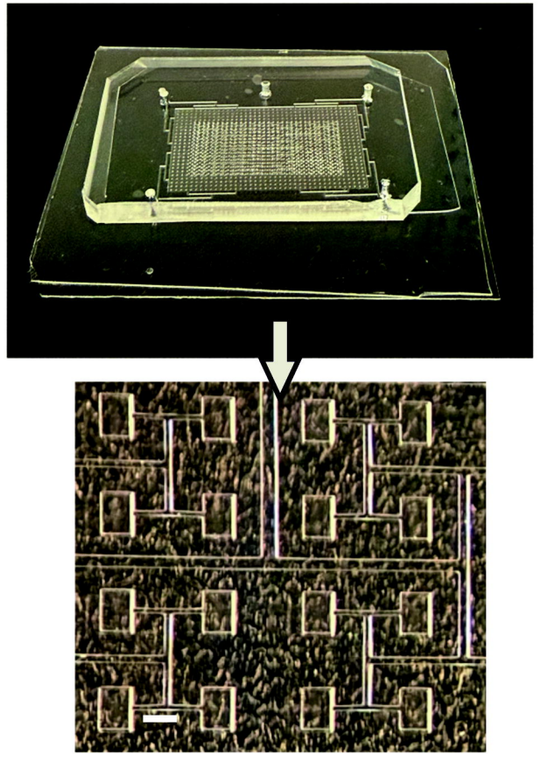

C

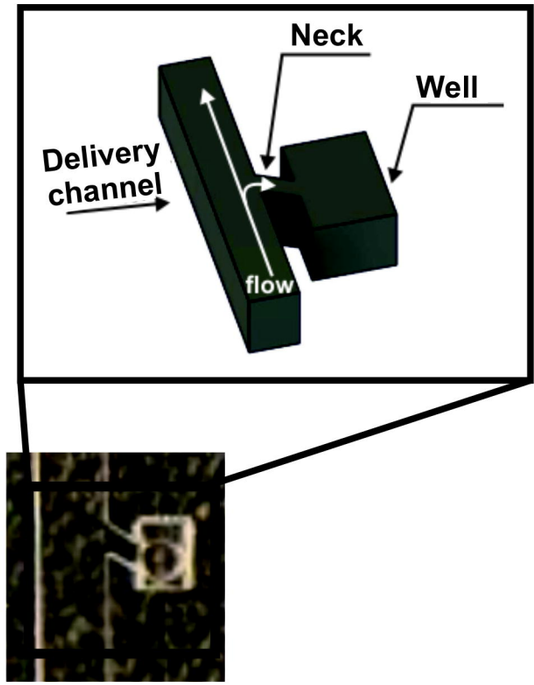

B

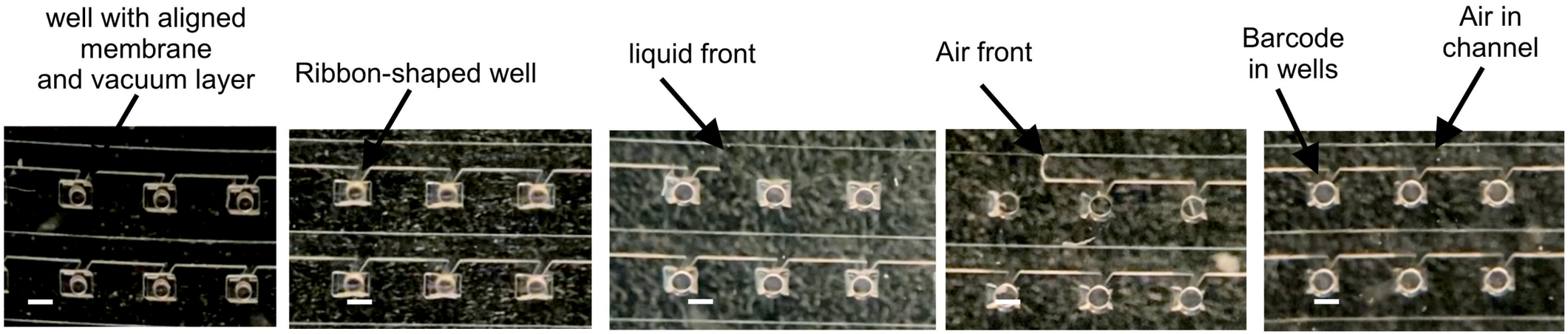

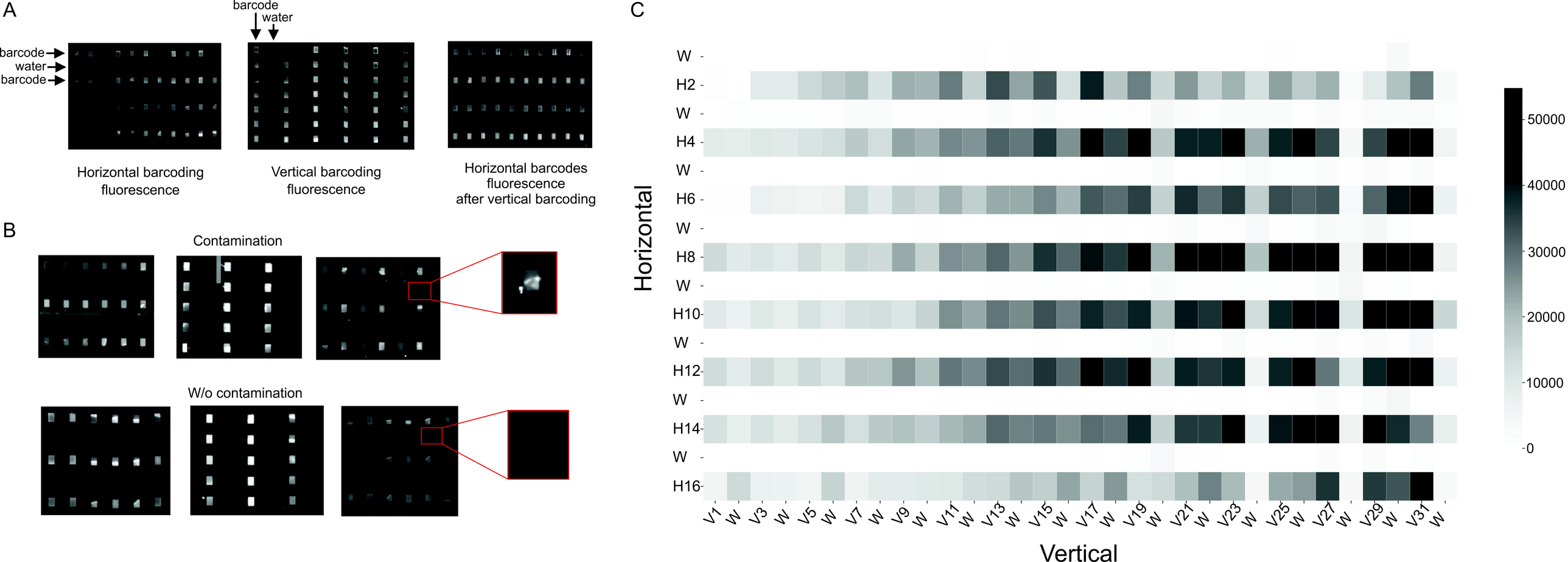
A
barcode
water
barcode
water
barcode
Horizontal barcoding fluorescence
Vertical barcoding fluorescence
Horizontal barcodes fluorescence after vertical barcoding
B
Contamination
W/o contamination
C
Horizontal
W
H2
H4
H6
H8
H10
H12
H14
H16
V1
V3
V5
V7
V9
V11
V13
V15
V17
V19
V21
V23
V25
V27
V29
V31
Vertical
50000
40000
30000
20000
10000
0

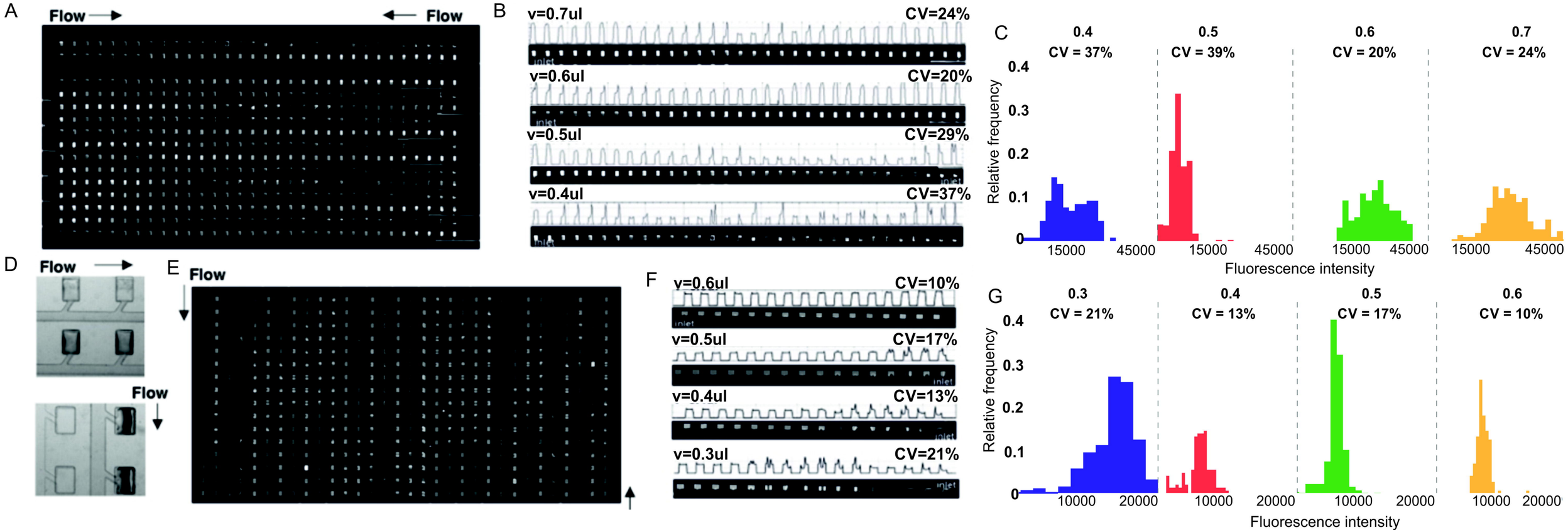
A
Flow
Flow
B
v=0.7ul
CV=24%
v=0.6ul
CV=20%
v=0.5ul
CV=29%
v=0.4ul
CV=37%
C
0.4
CV = 37%
0.5
CV = 39%
0.6
CV = 20%
0.7
CV = 24%
Relative frequency
Fluorescence intensity
D
Flow
Flow
E
Flow
F
v=0.6ul
CV=10%
v=0.5ul
CV=17%
v=0.4ul
CV=13%
v=0.3ul
CV=21%
G
0.3
CV = 21%
0.4
CV = 13%
0.5
CV = 17%
0.6
CV = 10%
Relative frequency
Fluorescence intensity